p-Wave Cold Collisions in an Optical Lattice Clock

N. D. Lemke,[1,*] J. von Stecher,[2] J. A. Sherman,[1] A. M. Rey,[2] C. W. Oates,[1] and A. D. Ludlow[1,†]

[1]*National Institute of Standards and Technology, Boulder, Colorado 80305, USA*
[2]*JILA, NIST, and University of Colorado, Department of Physics, Boulder, Colorado 80309, USA*
(Received 12 June 2011; published 30 August 2011)

We study ultracold collisions in fermionic ytterbium by precisely measuring the energy shifts they impart on the atoms' internal clock states. Exploiting Fermi statistics, we uncover *p*-wave collisions, in both weakly and strongly interacting regimes. With the higher density afforded by two-dimensional lattice confinement, we demonstrate that strong interactions can lead to a novel suppression of this collision shift. In addition to reducing the systematic errors of lattice clocks, this work has application to quantum information and quantum simulation with alkaline-earth atoms.

Ultracold alkaline-earth atoms trapped in an optical field are rich physical systems and attractive candidates for quantum information processing [1–4], quantum simulation of many-body Hamiltonians [5–9], and quantum metrology [10–14]. In each case, interrogating many atoms simultaneously facilitates high measurement precision, but can also yield high atomic density and the potential for atom-atom collisions at lattice sites with multiple atoms. For quantum information and simulation, these interactions can be a key feature; for quantum metrology, however, they present an undesired complication. For example, collisions can cause density-dependent frequency shifts in atomic clocks. In all cases, these interactions need to be well understood and controlled.

To limit interactions in lattice clocks, the use of ultra-cold, spin-polarized fermions was proposed to exploit the Fermi suppression of *s*-wave collisions while freezing out higher partial-wave contributions. This Fermi suppression arises from quantum statistics, which dictates that identical fermionic particles can collide only via odd partial waves. However, small collision shifts have been measured in fermionic ^{87}Sr ($I = 9/2$) [11,15,16] and ^{171}Yb ($I = 1/2$) [12], potentially compromising the ultimate accuracy of the lattice clocks. With ^{87}Sr it was found that *s*-wave collisions can occur even for initially indistinguishable fermions [15,17–19]. These collisions are enabled because the light-atom interaction introduces a degree of inhomogeneity, allowing the fermions to become slightly distinguishable. By contrast, using ^{171}Yb we highlight here the important role that *p*-wave collisions can play in fermionic lattice clock systems. Aided by quantum statistics, we present a complete picture of the cold collisions in the Yb lattice clock by performing measurements with state-of-the-art precision together with a quantitative theoretical model. Moreover, we demonstrate new techniques for canceling the collision shift that could be used to vastly reduce the clock uncertainty.

In order to simplify a complex system involving collisions of many lattice-trapped, two-level atoms interacting

with a laser field, we use two-pulse Ramsey spectroscopy [20] (Fig. 1) to probe the collision shift. Provided the pulse durations $t_{1,2}$ are short compared to the dark time between pulses T, the vast majority of the collisions occur while the atomic population is not being driven by the laser field. This simplifies our analysis by removing the time- and laser-detuning dependence of the excitation from the collisional dynamics. Additionally, with two dimensions of tight confinement and fewer atoms per lattice site, a 2D lattice allows the use of a 1D model for collisions between just two atoms in a regime where interactions are stronger.

Our model begins by considering this simple case: two atoms in the same lattice site, populating axial vibrational modes n_1 and n_2 and the lowest transverse band [4,5,18]. Assuming the vibrational quantum numbers are conserved during the collisions and laser interrogation, the Hamiltonian for the two-atom system can be written in a
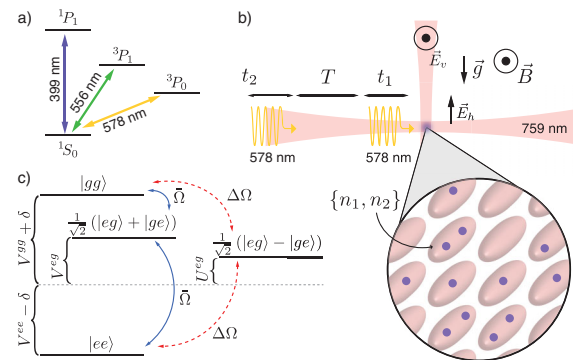

FIG. 1 (color).   (a) Energy level diagram for Yb. (b) Schematic of the two lattices. Arrows indicate optical polarizations and magnetic field directions with respect to gravity. At the left, the Ramsey pulse sequence is entering: two pulses of duration $t_{1,2}$ separated by dark time T (not to scale). An inset shows a few 2D lattice sites with 0 to 2 atoms per site; two atoms in one of the sites occupy axial motional states n_1 and n_2. (c) Energy level diagram for two atoms in the rotating frame: three triplet states and one singlet state, with interactions V and U, as in Eq. (1).

four-state basis set: $|gg\rangle$, $|ee\rangle$, $(|eg\rangle + |ge\rangle)/\sqrt{2}$ ("triplet states") and $(|eg\rangle - |ge\rangle)/\sqrt{2}$ ("singlet state") [16,17]. Here g and e are associated with the $^1S_0$ and $^3P_0$ electronic "clock" levels, respectively, which are coupled by the probe laser. Because the atomic population is prepared in a single nuclear-spin state ($m_I = 1/2$ or $-1/2$), quantum statistics dictates that only the triplet states, which are invariant under particle exchange, are affected by p-wave interactions, while the singlet configuration is affected by s-wave interactions only. The Hamiltonian in the rotating frame can be written in this basis as

$$H_T = \begin{pmatrix} \delta + V^{gg} & 0 & \bar{\Omega}/\sqrt{2} & \Delta\Omega/\sqrt{2} \\ 0 & -\delta + V^{ee} & \bar{\Omega}/\sqrt{2} & -\Delta\Omega/\sqrt{2} \\ \bar{\Omega}/\sqrt{2} & \bar{\Omega}/\sqrt{2} & V^{eg} & 0 \\ \Delta\Omega/\sqrt{2} & -\Delta\Omega/\sqrt{2} & 0 & U^{eg} \end{pmatrix}. \quad (1)$$

Here δ is the detuning from the atomic transition, $\bar{\Omega} = (\Omega_{n_1} + \Omega_{n_2})/2$ is the average Rabi frequency for the two atoms, and $\Delta\Omega = (\Omega_{n_1} - \Omega_{n_2})/2$ is the difference in Rabi frequency, which is nonzero in the presence of excitation inhomogeneity. The terms $U^{\alpha\beta}$ and $V^{\alpha\beta}$ give, respectively, the s- and p-wave interactions between an $\alpha = g$, e and a $\beta = g$, e atom occupying motional states n_1 and n_2 [21]. For short pulses and large Rabi frequencies ($\bar{\Omega} \gg U^{\alpha\beta}$, $V^{\alpha\beta}$), we can ignore collisions during the pulses. During the dark time, the Hamiltonian describing the atom dynamics is diagonal in the singlet-triplet basis, and each state acquires a phase shift. The different phase acquired by each state is what gives rise to the clock frequency shift.

The analytical solution for the frequency shift is cumbersome [21], but we gain insight by separately considering s- and p-wave interactions in a limiting case. p-wave interactions are fully allowed in the triplet manifold provided there is sufficient collision energy to overcome the centrifugal barrier (expected to exceed 30 μK based on calculated van der Waals coefficients [22]). For $\Delta\Omega = 0$, $t_1 = t_2$ and weak interactions $V^{\alpha,\beta}T \ll 1$ we obtain the simple expression (see [21])

$$\Delta\nu_p \sim \frac{V^{ee} - V^{gg} + (2V^{eg} - V^{ee} - V^{gg})(\frac{N_g - N_e}{2})}{4\pi}, \quad (2)$$

with N_g and N_e the ground and excited atom populations after the first pulse [23]. This expression is analogous to the one obtained for noncondensate bosons [24] and can be understood as the difference in chemical potential of the two components. In this simple limit the shift is independent of the dark time. Conversely, s-wave collision shifts occur only with excitation inhomogeneity ($\Delta\Omega \neq 0$). Again considering weak interactions ($U^{eg}T \ll 1$) and small inhomogeneity we find [17,18]

$$\Delta\nu_s \sim \left(\frac{\sin(\Delta\Omega t_1)}{\sin(\bar{\Omega} t_1)}\right)^2 \frac{U^{eg}(N_g - N_e)}{4\pi}. \quad (3)$$

While the relative sizes of the s- and p-wave shifts depend critically on the atomic scattering properties, which are generally not known, a simple estimate of the ratio between the s-wave and p-wave shifts can be made in free space [15]. Here, U^{eg} is proportional to the s-wave scattering length (a_{eg}) and independent of temperature ($\mathcal{T}$), while V scales as $k_T^2 b^3$, with b^3 the p-wave scattering volume and k_T the wave number associated with the thermal de Broglie wavelength ($k_T = \sqrt{2\pi m k_B \mathcal{T}}/\hbar$ with m the atom mass). Even for low temperature $\mathcal{T} = 1$ μK, with a moderate choice of scattering lengths $b \sim a_{eg} \sim 100 a_0$ (a_0 the Bohr radius) and a typical excitation inhomogeneity $\langle \Delta\Omega/\bar{\Omega}\rangle_{\mathcal{T}} \sim 0.1$, the ratio $\Delta\nu_p/\Delta\nu_s \sim 6$ reveals that neither type of interaction can be ignored [25].

In the 2D lattice, most sites are occupied by one or two atoms, and we expect the two-atom model [Eq. (1)] to correctly describe the physics, provided we integrate the shift over the spatial array of lattice sites. Moreover, instead of choosing a specific set of vibrational modes $\{n_1, n_2\}$, we numerically calculate the appropriate thermal average over all possible modes [21]. In the 1D lattice, each site is populated by many atoms, so the two-atom model is not directly applicable. However, in the weakly interacting regime, a mean-field picture that approximates many-atom interactions by a sum of pairwise interactions provides a fair description. Thus we use the two-atom Hamiltonian with temperature-dependent, effective interaction parameters to model the multiatom case. We compared this effective model with a numerically calculated N-body model and found qualitative agreement.

Our experimental procedures are similar to those described in [12]. After two stages of laser cooling [see Fig. 1(a)], atoms are trapped by the horizontal or vertical lattice for 1D confinement, or by both lattices for 2D operation. Approximately 25 000 atoms at temperature $\mathcal{T} \sim 10$ μK are trapped in the 1D lattice, which gives an estimated density of $\rho_1 = 3 \times 10^{11}/\text{cm}^3$ and an average of 20 atoms per site. In the 2D lattice, we estimate that 25% of the $\sim$5000 atoms are in doubly occupied sites, for which the effective density is $\rho_2 = 4 \times 10^{12}/\text{cm}^3$, and fewer than 1% of the atoms are in sites with more than two atoms. The lattice is tuned to the "magic wavelength" near 759 nm, where the two clock states experience identical trapping potentials. We offset the frequencies of the two lattice beams by 2 MHz using acousto-optic modulators, preventing any line broadening from the vector Stark shift [12,26–28]. With the atoms loaded in a lattice, we spin polarize the sample by optical pumping to one of the spin states ($m_F = \pm 1/2$) with 556 nm light; impurity in the spin polarization is $\leq 1\%$. The clock light, prestabilized to a high-finesse optical cavity [29] to be resonant with the $^1S_0 \rightarrow {}^3P_0$ clock transition, is switched on during the

Ramsey pulses with an acousto-optic modulator. The collision shift is found by repeatedly measuring the frequency offset between high- and low-density clock operations relative to the ultrastable optical cavity. These interleaved measurements have an instability of $\leq 1.5 \times 10^{-15}/\sqrt{\tau}$, for averaging time τ in seconds, allowing statistical error bars of ~ 20 mHz in just 2000 s.

We first considered the collision shift as a function of excitation fraction (i.e., the fraction in $^3P_0$ during the dark time). The excitation fraction was varied by changing the Rabi frequency of the Ramsey pulses. The measured shifts are shown in the blue and red points in Fig. 2(a) (1D lattice) and Fig. 2(b) (2D lattice). For these data, the pulse duration is $t_1 = t_2 = 1$ ms, and the dark time is $T = 80$ ms. For the 2D lattice the black dashed and solid red curves give the numerically calculated shift using the s-wave scattering length (a_{eg}^-) and p-wave scattering volumes (b_{eg}^3 and b_{ee}^3) as fitting parameters. (b_{gg} is taken to be zero, consistent with prior measurements [30].) For the 1D lattice, the curves are calculated from the mean-field approximation with the effective interaction parameters varied for fitting. Figure 2 shows that the p-wave interaction provides a much better description of the experimental data, as the shift induced by pure s-wave collisions is generally too small and does not exhibit the correct dependence on the excitation fraction. The shifts go through zero near an excitation fraction of 0.51 in the 1D lattice and 0.4 in the 2D lattice. Zero crossings near 0.5 are readily understood if V^{eg} dominates [see Eq. (2)]: by creating equal partial densities of ground and excited atoms ($N_g = N_e$), the energy shift on the two clock levels is the same, and the net shift is canceled. Operation of the clock at this zero crossing could substantially improve the performance of

the Yb system. The deviation from a zero crossing at exactly 0.5 in the 1D case is consistent with a small ee interaction ($V^{ee} \approx 0.1 V^{eg}$).

To further rule out s-wave interactions, we misaligned the probe beam to couple more strongly to the weak confinement axis of the lattice trap [Fig. 2(c)]. Doing so introduces greater excitation inhomogeneity from the Ramsey pulse (in this case, up to a factor of 2.4) because the atoms are not tightly confined along this axis [15]. We expect the s-wave shift to depend quadratically on the inhomogeneity, yet the frequency shifts show no change. This insensitivity is well explained by p-wave interactions, which depend only weakly on inhomogeneity at these levels (decreasing slightly as more population transfers to the singlet state). A small but nonzero s-wave interaction could balance this effect and may help explain the complete lack of dependence, as shown in the theory curves in Fig. 2(c). The green long-dashed lines in Figs. 2(a) and 2(b) also show that adding a small but nonzero s-wave interaction is consistent with the observed collision shifts. Still, all of these considerations indicate that p-wave interactions play the dominant role in the cold collisions of ^{171}Yb.

We experimentally investigated several effects not included in the model to ascertain their importance. First, we explored the role of tunneling by measuring the shifts for both vertically and horizontally oriented 1D lattices, exploiting gravity-induced suppression of the tunneling rate [21,31], but we observed no change in the data [Fig. 2(a)]. A second effect, laser-induced mode-changing collisions, can occur for pulses shorter than the mean oscillation period in the trap. Nevertheless, we ruled out the relevance of those processes by varying the pulse duration over a factor of 10 without observing any substantial modification to the measured
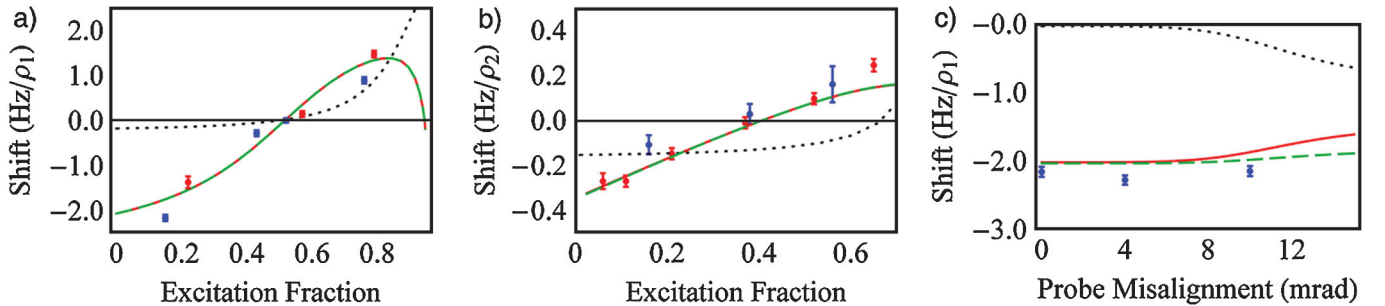

FIG. 2 (color). (a) Collision shift vs excitation fraction, 1D lattice. Blue (red) points show experimental measurements in a vertical (horizontal) lattice with temperature $\mathcal{T} \sim 10~\mu$K and $\langle \Delta\Omega/\bar{\Omega} \rangle_{\mathcal{T}} = 0.2$. Dashed black line gives an s-wave-only fit ($\langle U^{eg} \rangle_{\mathcal{T}} = -2\pi \times 3.0$ Hz) from the mean-field model. Solid red line gives a p-wave-only fit with $\langle V^{eg} \rangle_{\mathcal{T}} = 10\langle V^{ee} \rangle_{\mathcal{T}} = -2\pi \times 2.2$ Hz. Long-dashed green line adds to this a small s-wave component ($\langle U^{eg} \rangle_{\mathcal{T}} = -2\pi \times 1.2$ Hz). (b) Collision shift vs excitation fraction, 2D lattice. Blue (red) points show experimental measurements probing along the vertical (horizontal) direction. Dashed black line is an s-wave-only fit with $a_{eg}^- \approx -25~a_0$ (a_0 the Bohr radius); solid red line is a p-wave-only fit with $b_{eg} \approx -74~a_0$ and $b_{ee}^3 = 0.1 b_{eg}^3$. The long-dashed green line adds to this a small s-wave interaction $a_{eg}^- = -25~a_0$. We emphasize that these are not necessarily accurate determinations of the scattering lengths since their values depend on the spatial distribution of the atoms in the 2D lattice, which is not well characterized. (c) Collision shift vs probe misalignment angle (vertical 1D lattice) for constant excitation fraction 0.12. Using the same parameters as (a), the dashed black line gives an s-wave-only fit, solid red line gives a p-wave-only fit, and the long-dashed green line has s- and p-wave terms. In the well-aligned case (0 mrad) there is a residual effective misalignment of ~ 5 mrad due to the imperfect overlap between lattice and probe beams.
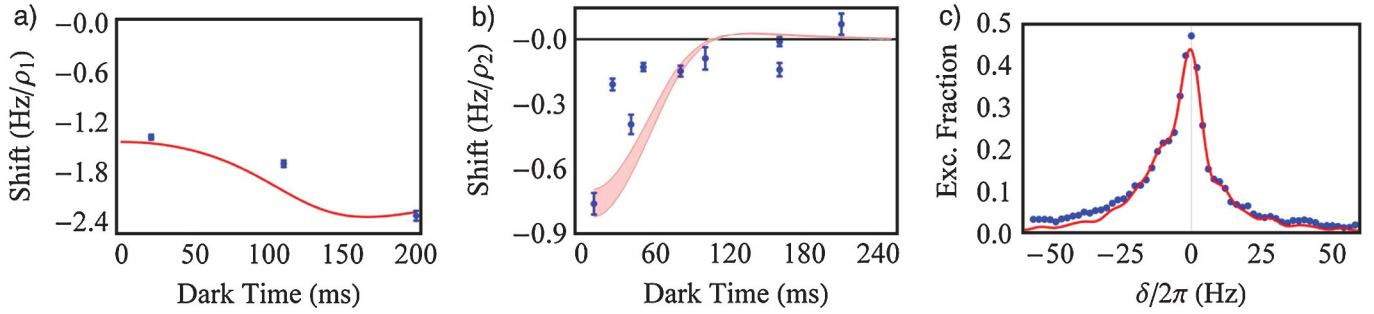
FIG. 3 (color).   (a) Collision shift vs dark time, 1D lattice, for excitation fraction 0.18. Using the same parameters as Fig. 2(a), the solid line gives a fit from the mean-field model. (b) Collision shift vs dark time, 2D lattice, for excitation fraction $0.19 \pm .03$. The shift crosses zero due to the periodic dependence of the shift on collisional phase, and is a signature of strong interactions. The model calculations (shaded region) use the same parameters as Fig. 2(b) for an excitation fraction range $0.19 \pm .03$. (c) Asymmetric Rabi spectrum, 2D lattice. The solid line is the prediction of the model, using the number of doubly occupied sites as a fitting parameter.

collision shifts [21]. Finally, we note that we looked for dependence of the collision shifts on the second pulse area [17], and found no significant dependencies.

It is interesting to see how collision effects are manifest in a regime of high density and strong interactions (e.g. $V^{\alpha,\beta}T \geq 1$). A key observation revealing the operation of the 2D lattice clock in the regime $V^{ge}T \gg V^{ee}T \geq 1$ is the zero crossing of the collision shift at a lower excitation fraction of 0.4, which deviates from the crossing near 0.5 found for weak interactions [Fig. 2(a) and Eq. (2)]. This change occurs due to the nontrivial counterplay between V^{ge} and V^{ee} in the strongly interacting regime. The interaction strength also introduces additional dependencies on the dark time. As mentioned previously, the shift is independent of T for weak interactions, but with strong interactions it decays with increasing T due to the shift's sinusoidal dependence on scattering phase [21,32]. We investigated this experimentally by varying the dark time T and measuring collision shifts in the 1D lattice [Fig. 3(a)], where the shift scales weakly with T, and the 2D lattice [Fig. 3(b)], where the shift is strongly damped towards zero with increasing T. Yet a third signature of strong interactions is significant asymmetry in the clock transition spectrum. In Fig. 3(c) we show a Rabi spectrum ($t = 120$ ms), taken under high density operation in the 2D lattice, which shows an additional feature on the red side ($\delta < 0$) of resonance. This asymmetry is density dependent and less observable in the 1D lattice. In the 2D lattice, the interactions are sufficiently strong ($V^{eg}t \geq 1$) to introduce these asymmetric line shape features beyond the transition linewidth. With yet higher density, it may be possible to spectrally resolve three features, one each for the s-wave-interacting singlet, the p-wave-interacting triplets, and the noninteracting atoms in singly occupied lattice sites. Interaction-induced sidebands were recently reported in [33] and may be useful for quantum simulation applications.

In this Letter we have shown evidence for p-wave interactions in ultracold Yb confined in an optical lattice. Although lower atomic temperature yields reduced

tunneling through the p-wave barrier, and thus a lower scattering cross section, it also increases the atomic density of the confined atoms. Depending on the detailed scattering parameters, both s- and p-wave interactions may be relevant for all optical lattice clock systems. Using the dependence of the measured shift on excitation fraction and dark time, we have observed zero crossings in the measured frequency shifts, which provide the metrological means to reduce the shifts to nearly negligible levels.

*Also at Department of Physics, University of Colorado, Boulder, CO 80309, USA.
†ludlow@boulder.nist.gov

[1] D. Hayes, P. S. Julienne, and I. H. Deutsch, Phys. Rev. Lett. **98**, 070501 (2007).
[2] I. Reichenbach and I. H. Deutsch, Phys. Rev. Lett. **99**, 123001 (2007).
[3] A. J. Daley, M. M. Boyd, J. Ye, and P. Zoller, Phys. Rev. Lett. **101**, 170504 (2008).
[4] A. V. Gorshkov et al., Phys. Rev. Lett. **102**, 110503 (2009).
[5] A. V. Gorshkov et al., Nature Phys. **6**, 289 (2010).
[6] M. A. Cazalilla, A. F. Ho, and M. Ueda, New J. Phys. **11**, 103033 (2009).
[7] M. Foss-Feig, M. Hermele, and A. M. Rey, Phys. Rev. A **81**, 051603 (2010).
[8] M. Foss-Feig, M. Hermele, V. Gurarie, and A. M. Rey, Phys. Rev. A **82**, 053624 (2010).
[9] M. Hermele, V. Gurarie, and A. M. Rey, Phys. Rev. Lett. **103**, 135301 (2009).
[10] H. Katori, M. Takamoto, V. G. Pal'chikov, and V. D. Ovsiannikov, Phys. Rev. Lett. **91**, 173005 (2003).
[11] A. D. Ludlow et al., Science **319**, 1805 (2008).
[12] N. D. Lemke et al., Phys. Rev. Lett. **103**, 063001 (2009).
[13] R. Le Targat et al., Phys. Rev. Lett. **97**, 130801 (2006).

[14] T. Akatsuka, M. Takamoto, and H. Katori, Nature Phys. **4,** 954 (2008).

[15] G. K. Campbell *et al.*, Science **324,** 360 (2009).

[16] M. D. Swallows *et al.*, Science **331,** 1043 (2011).

[17] K. Gibble, Phys. Rev. Lett. **103,** 113202 (2009).

[18] A. M. Rey, A. V. Gorshkov, and C. Rubbo, Phys. Rev. Lett. **103,** 260402 (2009).

[19] Z. Yu and C. J. Pethick, Phys. Rev. Lett. **104,** 010801 (2010).

[20] N. F. Ramsey, Phys. Rev. **78,** 695 (1950).

[21] See Supplemental Material at http://link.aps.org/supplemental/10.1103/PhysRevLett.107.103902 for further details of the theoretical model and experimental parameters.

[22] V. A. Dzuba and A. Derevianko, J. Phys. B **43,** 074011 (2010).

[23] Note that $(N_g - N_e)/(N_g + N_e) = \cos(\bar{\Omega}t_1)$.

[24] D. M. Harber, H. J. Lewandowski, J. M. McGuirk, and E. A. Cornell, Phys. Rev. A **66,** 053616 (2002).

[25] In a trapping potential, this ratio can be even larger since k_T is modified by the zero-point energy of the trap.

[26] S. G. Porsev, A. Derevianko, and E. N. Fortson, Phys. Rev. A **69,** 021403 (2004).

[27] C. Chin *et al.*, Phys. Rev. A **63,** 033401 (2001).

[28] J. Sebby-Strabley, M. Anderlini, P. S. Jessen, and J. V. Porto, Phys. Rev. A **73,** 033605 (2006).

[29] Y. Y. Jiang *et al.*, Nat. Photon. **5,** 158 (2011).

[30] M. Kitagawa *et al.*, Phys. Rev. A **77,** 012719 (2008).

[31] P. Lemonde and P. Wolf, Phys. Rev. A **72,** 033409 (2005).

[32] K. Gibble, *IEEE International Frequency Control Symposium* (IEEE, New York, 2010), pp. 56–58.

[33] M. Bishof *et al.*, Phys. Rev. Lett. **106,** 250801 (2011).